SIAM J. APPL. MATH.
Vol. 67, No. 2, pp. 364–386

AN ASYMPTOTIC FRAMEWORK FOR FINITE HYDRAULIC FRACTURES INCLUDING LEAK-OFF*

S. L. MITCHELL†, R. KUSKE†, AND A. P. PEIRCE†

Abstract. The dynamics of hydraulic fracture, described by a system of nonlinear integro-differential equations, is studied through the development and application of a multiparameter singular perturbation analysis. We present a new single expansion framework which describes the interaction between several physical processes, namely viscosity, toughness, and leak-off. The problem has nonlocal and nonlinear effects which give a complex solution structure involving transitions on small scales near the tip of the fracture. Detailed solutions obtained in the crack tip region vary with the dominant physical processes. The parameters quantifying these processes can be identified from critical scaling relationships, which are then used to construct a smooth solution for the fracture depending on all three processes. Our work focuses on plane strain hydraulic fractures on long time scales, and this methodology shows promise for related models with additional time scales, fluid lag, or different geometries, such as radial (penny-shaped) fractures and the classical Perkins–Kern–Nordgren (PKN) model.

Key words. asymptotic solutions, crack tip, critical scales, hydraulic fractures, integral-differential equations, leak-off

AMS subject classifications. 45K05, 35A20, 35B40, 76D08, 74B05, 74R10

DOI. 10.1137/04062059X

1. Introduction.

Hydraulic fractures are propagated in an elastic material due to the pressure exerted by a viscous fluid on the fracture. These fractures occur naturally in volcanic dikes where magma causes fracture propagation below the surface of the earth [37, 38, 55]. In the oil and gas industry hydraulic fractures are deliberately propagated in reservoirs to increase production. Hydraulic fracture models need to account for the primary physical mechanisms involved: deformation of the rock, fracturing of the rock, flow of viscous fluid within the fracture, and leak-off of the fracturing fluid into the permeable rock. The parameters that characterize these processes are, respectively, Young's modulus E and Poisson's ratio ν, the rock toughness K_{Ic}, the fluid viscosity μ, and the leak-off coefficient C_l.

The challenges for analysis of these models originate from the nonlinearity of the equation describing the flow of fluid in the fracture, the nonlocal character of the elastic response of the fracture, and the history-dependence of the equation governing the exchange of fluid between the fracture and the rock. The singular tip behavior, which can be difficult to resolve numerically, dominates these solutions and is highly dependent on the relative importance of the contributing physical processes. Therefore, the objectives of analytic treatment of these models are as follows: to characterize the structure of the near-tip solution that can be embedded in numerical algorithms, to provide benchmark solutions to test numerical codes, and to determine the parameter values and length scales that characterize the transitions between distinct combinations of physical processes. In this paper we use a novel asymptotic framework that enables us to characterize the different propagation regimes and provide asymptotic solutions when more than two physical processes are competing simultaneously. This

*Received by the editors December 9, 2004; accepted for publication (in revised form) August 14, 2006; published electronically January 12, 2007.
http://www.siam.org/journals/siap/67-2/62059.html
†Department of Mathematics, University of British Columbia, Vancouver, BC, V6T 1Z2, Canada (sarah@iam.ubc.ca, rachel@math.ubc.ca, peirce@math.ubc.ca).

is distinct from previous analytic work on such models, which have been restricted to considering at most two competing physical processes [6, 23, 24, 26].

There has been a significant amount of work in the last half century involving the mathematical modeling of hydraulic fractures [1, 8, 14, 28, 30, 31, 32, 33, 45, 48, 55]. As discussed in [21] and the references therein, the aim of these models is to calculate the fluid pressure, opening, and size of the fracture given the properties of the rock, the injection rate, and the fluid characteristics. More recent work has been concerned with developing numerical algorithms to simulate three-dimensional propagation of hydraulic fractures in layered strata [5, 7, 12, 46, 47, 53]; this is in contrast to earlier work where approximate solutions were found for simple fracture geometries [1, 8, 28, 33, 45, 48, 55]. A substantial difference between hydraulic fracturing and other studies of fracture (see [22, 49, 52]) is the coupling with the equations for the fluid and fracture geometry. Most models in hydraulic fracturing only consider planar fractures rather than kinked or curved cracks [13, 41, 42].

The relevant fracture geometry that we consider in this paper, known as the KGD (plane strain) model, was developed independently by Khristianovic and Zheltov [33] and Geertsma and de Klerk [28]. The fracture is assumed to be an infinite vertical strip so that horizontal cross-sections are in a state of plane strain. This model is applicable to large aspect ratio rectangular planar fractures and was extended in [54] to include toughness. A major contribution to this mathematical modeling was made by Spence and Sharp [54], who initiated the work on self-similar solutions and scaling for a KGD crack propagating in an elastic, impermeable medium with finite toughness. This approach has been continued through asymptotic analyses of near-tip processes, yielding the results from [15] for zero toughness in an impermeable rock, and from [36] for zero toughness when leak-off is dominant. Several papers [16, 19, 27] have extended this analysis to include toughness and fluid lag, where regions devoid of fluid develop close to the crack tip, along with transitional regions. In this paper we assume that fluid lag is negligible and so these effects can be ignored.

Certain phases of hydraulic fracture propagation are characterized within a dimensionless parametric space [21, 20], with boundaries controlled by the dominant processes, namely, viscosity, toughness, or leak-off. This framework has been the basis for semianalytical solutions for simple geometries (KGD and penny-shaped) and benchmarks for numerical simulators. These include the following asymptotic regimes: impermeable with zero toughness [2, 10, 50], small toughness [24], finite toughness [3, 54], and large toughness [26, 50]; and permeable with zero toughness [4].

Since much of our analysis is closely related and complementary to these most recent studies, we outline the context here, with further discussion given in section 1.1 in terms of the specific model. Previous analyses [2, 9, 10, 24, 25, 26, 27] have been limited to parameter regimes where one or two physical processes dominate the dynamics, with the remainder of the related nondimensional quantities set to unity. In each case there is a different set of scaling parameters defined, depending on the dominant process(es), corresponding to the edges and corners of the parameter space [6, 21]. These methods lead to asymptotic expansions for the tip behavior, where the terms in the expansion involve powers of the distance from the tip. In the case of vanishing leak-off, this method has also been used to describe the transition in behavior between different power law expansions [2]. Recent preliminary studies [23, 34, 35] have also used combinations of power law expansions in the context of a semi-infinite approximation for the fracture, combined with numerical methods to understand transitions between different scaling regimes.

In this paper we present a unifying scaling framework based on singular perturbation techniques which analyzes how the physical processes, namely, viscosity, toughness, and leak-off, all influence the KGD crack behavior. Avoiding semi-infinite approximations, it involves the simultaneous scaling of all three processes relative to the distance from the fracture tip: this means that the approach is applicable for different combinations of the dominant physical processes. It has been used in [44] for the impermeable case in which only the processes of viscous dissipation and energy release compete. Thus it provides a construction of the solution in the crucial tip region, identifying the parameter combinations which quantify spatial transitions in the behavior of the fracture. The scaling exponents of the physical processes are determined as part of the method, so that it can be applied to construct approximate solutions in intermediate parameter regimes where several processes are in balance. The resulting asymptotic approximation provides verification of the conditions under which self-similar solutions are appropriate, and indicates regimes in which a more complicated time-dependence is involved, as discussed in section 4. We also briefly outline how the technique can be generalized to regimes where there is more than one transition in the behavior near the tip.

The fracture propagation is formulated as a system of coupled integrodifferential equations, and our method proves to be very beneficial in understanding the nonlocal and local effects that arise. It can be applied to different geometries, such as the classical Perkins–Kern–Nordgren (PKN) model [43], and we expect that it can be extended to model other effects such as stress jumps and fluid lag.

1.1. Problem formulation and dimensional results. The solution of the KGD hydraulic fracture problem (shown in Figure 1.1) consists of determining the fracture opening w and the net pressure p (the difference between the fluid pressure p_f and the far-field stress σ_o) as functions of space and time, as well as the fracture half-length, $l(t)$. These functions depend on the volumetric fluid injection rate Q_0, assumed constant in this paper, and on the four material parameters E', μ', K', and

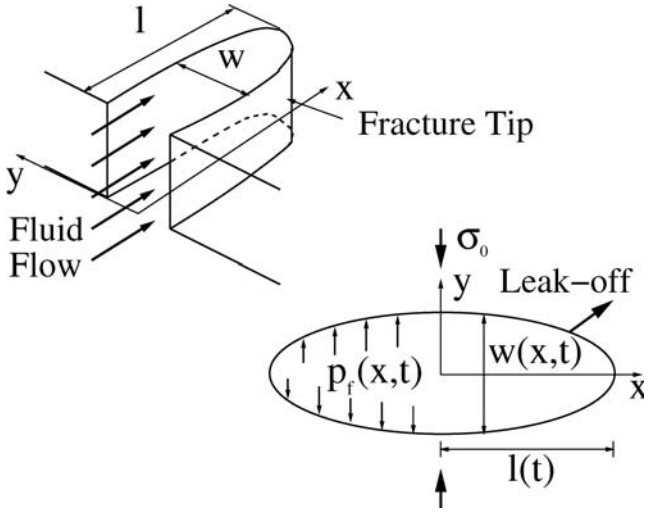

FIG. 1.1. *Diagrams showing the KGD crack and its cross-section.*

C', respectively, defined as

$$E' = \frac{E}{1-\nu^2}, \qquad \mu' = 12\mu, \qquad K' = 4\left(\frac{2}{\pi}\right)^{1/2} K_{Ic}, \qquad C' = 2C_l, \tag{1.1}$$

which are combinations of the parameters quantifying the primary physical mechanisms described at the beginning of this section. The rock toughness K_{Ic} is assumed to be equal to the stress intensity factor K_I which, for this geometry, can be expressed as an integral of the pressure

$$K_{Ic} = K_I = 2\sqrt{\frac{l}{\pi}} \int_0^l \frac{p}{\sqrt{l^2 - x^2}}\, \mathrm{d}x. \tag{1.2}$$

The equations for the KGD fracture are as follows:

$$\text{Reynolds' (lubrication) equation:} \quad \frac{\partial w}{\partial t} + g = \frac{1}{\mu'} \frac{\partial}{\partial x}\left[w^3 \frac{\partial p}{\partial x}\right] + Q_0 \delta(x), \tag{1.3}$$

which describes the conservation of fluid mass for an incompressible fluid. Note that g is the leak-off term which describes the fluid infiltration into the surrounding rock.

$$\text{Elasticity equation:} \qquad p(x,t) = -\frac{E'}{4\pi} \int_{-l}^{l} \frac{\partial w}{\partial s} \frac{\mathrm{d}s}{s-x}, \tag{1.4}$$

which describes the balance of forces and is a nonlocal equation relating the fracture opening w and net pressure p for a state of plane strain.

$$\text{Propagation condition:} \quad w = \frac{K'}{E'}\sqrt{l-x} + O\big[(l-x)^{3/2}\big], \qquad x \longrightarrow \pm l, \tag{1.5}$$

which accounts for the energy required to break the rock and is the condition that the fracture is in mobile equilibrium.

$$\text{Boundary conditions:} \qquad w = 0, \qquad w^3 \frac{\partial p}{\partial x} = 0, \qquad \text{at } x = \pm l. \tag{1.6}$$

$$\text{Global volume balance condition:} \quad Q_0 t = \int_{-l}^{l} w(s,t)\, \mathrm{d}s + \int_0^t \int_{-l}^{l} g(s,\tau)\, \mathrm{d}s\, \mathrm{d}\tau, \tag{1.7}$$

which equates the crack volume to the volume of injected fluid and amount lost to the surrounding rock mass, obtained by integrating (1.3) and applying (1.6). If $t_0(x)$ is the time at which the crack tip arrived at the point x, and t is the current time, then the leak-off function g is defined as

$$\text{Carter's leak-off model:} \qquad g(x,t) = \frac{C' H(t - t_0)}{\sqrt{t - t_0(x)}}. \tag{1.8}$$

The memory term $t_0(x)$ implies that the leak-off function $g(x,t)$ depends on the entire history of the fracture front locations, which significantly complicates the analysis.

Since its introduction in 1957, Carter's leak-off model [11] has been widely accepted and successfully used in the oil and gas industry to design hydraulic fracturing

treatments and has been referred to as "the standard model of fracturing fluid loss" (see [36]). We briefly summarize the steps involved in the derivation of the model and discuss its applicability for high confinement geological situations, which are becoming more important as deeper reserves are being exploited.

The first assumption made in the derivation of Carter's leak-off model is that the hydraulic load $\Delta p = p_f - p_0$ driving the leak-off process is approximately constant, where p_0 is the reservoir pore pressure. This assumption can be justified in high confinement reservoirs where $p_f \approx \sigma_0 \gg p_0$. In this case the hydraulic load is much larger than the net pressure $p = p_f - \sigma_0$ and is approximately constant, i.e., $\Delta p \approx \sigma_0 - p_0$. The second assumption made in the derivation of (1.8) is in approximating the leak-off process by a one-dimensional flow perpendicular to the crack propagation axis that does not account for any lateral interaction. Modeling this gradient-driven flow involves incorporating the growth of an impermeable *filter cake* layer via the deposition of polymer molecules by the leaking fluid, the growth of an *invaded zone* of fluid that penetrates the filter cake, and a pressure diffusion zone within the reservoir. Combining these three physical processes in series yields (1.8), in which the lumped coefficient C' is known as the *Carter leak-off coefficient* (see [6, 11, 39, 51] and the references therein).

Assuming that $l(t) = at^{1/2}$, Gordeyev and Entov [29] derived a similarity solution to the two-dimensional pressure diffusion equation, which yields a leak-off velocity of the same form as (1.8). In this case the fracture is growing sufficiently rapidly for the leak-off process to be one-dimensional, a situation that is likely to persist for power laws in which the fracture evolves more rapidly: $l(t) = at^{\lambda}$, where $\lambda \geq \frac{1}{2}$. Carter's model (1.8), which is based on the pressure diffusion equation, ignores feedback coupling between the reservoir pressure field and the elastic strain in the rock. This pure diffusion approximation can be justified using poroelasticity theory [17, 18] in which the elastic strain feedback due to the hydraulic load Δp is shown to vanish identically. Moreover, for high confinement reservoirs the mechanical load effect (due to the net pressure p which forces the crack to open) on the reservoir pressure is insignificant compared to that of the hydraulic load, since $\Delta p \gg p$.

There may be a question as to the validity of Carter's model right at the crack tip. However, the analysis presented in this paper is based on the fact that the dominant physical process governing the behavior of the fracture at the tip, which we refer to as the *near-tip region*, is the energy released in the breaking of the rock as characterized by the fracture toughness. Since the leak-off process is subdominant to this and only manifests itself a distance away from the tip in the *intermediate-tip region*, we make use of the model only in a region where it is still valid. We could include other higher order effects to model the leak-off more carefully in the near-tip region, but this is neglected in our analysis since it is not the dominant process.

The method presented in this paper involves an iterative construction of the asymptotic solution: the lubrication and elasticity equations (1.3)–(1.4) alternatively give the form of the solution. The volume balance equation (1.7) is applied to complete the solution: it verifies the balance of physical processes, determines unknown constants, and provides a consistency check on the temporal behavior of the solution. The propagation condition (1.5) manifests itself in the asymptotic behavior of the tip when the influence of the toughness is dominant; this depends on the relative scalings of the parameters and the distance from the tip.

We give the main results for w in terms of the dimensional variables; the expansions for p can then be determined from (1.4). For $\mathcal{P}_{ckm} \gg (\ll) (1-\xi)^{1/2}$, respectively,

we find that

$$w \sim \frac{K'}{E'} l^{1/2} \left\{ \left(1 - \frac{x}{l}\right)^{1/2} + \left[\frac{8\pi}{3}\gamma^{3/2}\mathcal{P}_{km}^{-1} + 4\sqrt{2}\pi\gamma\mathcal{P}_{ckm}^{-1}\right]\left(1 - \frac{x}{l}\right)\right\}, \tag{1.9}$$

$$w \sim \left(\frac{C'\mu'}{E'}\right)^{1/4} \frac{l^{3/4}}{t^{1/8}}\gamma^{-3/4}\left\{\tilde{C}_{01}\left(1 - \frac{x}{l}\right)^{5/8} + \mathcal{B}_1\left(1 - \frac{x}{l}\right)^{1/8} + \mathcal{B}_2\mathcal{P}_{cm}^{-1/4}\left(1 - \frac{x}{l}\right)^{3/4} + \mathcal{B}_3\left(1 - \frac{x}{l}\right)^{r}\right\}, \tag{1.10}$$

where $\tilde{C}_{01}$, $\mathcal{B}_1$, $\mathcal{B}_2$, $\mathcal{B}_3$, and r are constants determined in the solution process, and γ is an $O(1)$ quantity introduced in the rescaling below. The three key parameter combinations

$$\mathcal{P}_{km} := \frac{K'^3}{\mu' E'^2}\frac{\gamma^{3/2}t}{l^{3/2}}, \qquad \mathcal{P}_{cm} := \frac{C'^3 E'}{\mu'}\frac{\gamma^3 t^{5/2}}{l^3}, \qquad \mathcal{P}_{ckm} := \frac{K'^4}{C'\mu' E'^3}\frac{\gamma t^{1/2}}{l} \tag{1.11}$$

characterize the different behavior regimes, as shown in the analysis. The leading order term in (1.10) was established by [36] for the stationary solution and then confirmed in [6] for zero toughness. In a preliminary study [9], which considers the infinite limit of a nondimensional parameter for the volume of injected fluid (2.2), the first and last terms in both (1.9) and (1.10) are also determined. However, the other terms are not found there, since certain parameter combinations are fixed (see section 3.2 for further discussion.) These additional terms allow us to analytically construct a uniform solution near the tip, instead of numerically as in [24] for zero leak-off. Near and far-field solutions for semi-infinite approximations of the fracture [23, 35, 34] also use expansions in powers of $(1-\xi)$, which include some of the powers from (1.9)–(1.10) in addition to other terms related to the semi-infinite limit. Power law expansions similar to (1.9)–(1.10) for the zero leak-off case are derived in [44]. Some of these terms are also determined in [6, 24], but the additional terms found in [44] allow the uniform tip behavior to be constructed analytically.

The asymptotic expansions (1.9)–(1.10) explicitly identify the critical parameter combinations (1.11) that dictate transitions between (1.9) and (1.10) in the tip vicinity. These quantities are combinations of the dimensionless parameters that arise in the rescaling below, which quantify the physical processes viscosity, toughness, and leak-off. From the construction of expansions (1.9)–(1.10) we can understand the changes in tip behavior as we scale the quantities (1.11) with a parameter related to the distance from the tip $\xi = 1$. Our method does not use a semi-infinite approximation, and therefore can be extended to study additional time dependencies, transients, and other types of hydraulic fractures, such as finger-like geometries, known as the PKN fracture [45, 48].

In section 2 we describe the new approach and in section 3 obtain expansions when all three processes play a role, in the case that leak-off dictates the leading order behavior. The construction leads to the identification of the parameter combinations (1.11) which are necessary for describing the transition between the near- and intermediate-tip solutions (1.9)–(1.10). Section 4 summarizes our results and briefly outlines extensions of our methodology to situations where time-dependence must be scaled explicitly, or cases where there is more than one transition in the dominant shape of the fracture.

2. Approach of the new method. We introduce the nondimensional quantities, following [6, 26, 24] and others:

$$\xi = x/l, \qquad l = L\gamma, \qquad w = \epsilon L\Omega, \qquad p = \epsilon E'\Pi. \tag{2.1}$$

It is convenient to work with the dimensionless quantities Ω (the opening), Π (the net pressure), and γ (a fracture length), which are all $O(1)$. The parameter ϵ is used in [6, 26, 24] to relate w/l to p/E', so for comparison purposes we include it in our analysis; however, it plays no role here and so could be set to unity. Also, L denotes a length scale and is of the same order as the fracture length l.

We also define four nondimensional quantities,

$$\mathcal{G}_v = \frac{Q_0 t}{\epsilon L^2}, \qquad \mathcal{G}_m = \frac{\mu'}{\epsilon^3 E' t}, \qquad \mathcal{G}_k = \frac{K'}{\epsilon E' L^{1/2}}, \qquad \mathcal{G}_c = \frac{C' t^{1/2}}{\epsilon L}, \tag{2.2}$$

and determine different solutions depending on the size of combinations of these parameters (1.11) without setting any to unity. The governing equations (1.3)–(1.7) are now

$$\frac{t(\epsilon L)_t}{\epsilon L}\Omega + \dot{\Omega} t - \xi \frac{t(L\gamma)_t}{L\gamma}\frac{\partial \Omega}{\partial \xi} + \mathcal{G}_c \Gamma_l = \frac{1}{\mathcal{G}_m}\frac{1}{\gamma^2}\frac{\partial}{\partial \xi}\left[\Omega^3 \frac{\partial \Pi}{\partial \xi}\right], \tag{2.3}$$

$$\Pi = -\frac{1}{4\pi\gamma}\int_{-1}^{1} \frac{\partial \Omega}{\partial \chi}\frac{\mathrm{d}\chi}{\chi - \xi}, \tag{2.4}$$

$$\Omega = \mathcal{G}_k \gamma^{1/2}(1 \mp \xi)^{1/2}, \quad \xi \longrightarrow \pm 1; \qquad \Omega = 0, \quad \Omega^3 \frac{\partial \Pi}{\partial \xi} = 0, \quad \text{at } \xi = 1^{\pm}, \tag{2.5}$$

$$\mathcal{G}_v = \gamma \int_{-1}^{1} \Omega \, \mathrm{d}\chi + \mathcal{G}_c \frac{1}{L}\int_0^1 l(\theta t)\theta^{-1/2} \int_{-1}^{1} \Gamma_l \, \mathrm{d}\chi \, \mathrm{d}\theta, \tag{2.6}$$

where Γ_l is the dimensionless leak-off function discussed below.

The new approach relies on two main ingredients: (i) a scaling parameter $\delta \ll 1$ that relates distance from the tip to the key dimensionless quantities in (2.2), and (ii) a flexible asymptotic expansion which can handle behavior dominated by different physical quantities. Thus we define

$$1 - \delta z = \xi, \tag{2.7}$$

$$\mathcal{G}_v = \delta^{\beta_v}\hat{\mathcal{G}}_v, \quad \mathcal{G}_k = \delta^{\beta_k}\hat{\mathcal{G}}_k, \quad \mathcal{G}_m = \delta^{\beta_m}\hat{\mathcal{G}}_m, \quad \mathcal{G}_c = \delta^{\beta_c}\hat{\mathcal{G}}_c, \tag{2.8}$$

where the $\hat{\mathcal{G}}_{()}$'s are $O(1)$ quantities. The different regimes are then characterized by inequalities between the values of the exponents β_v, β_k, β_m, β_c. Here δ is introduced as a bookkeeping parameter that disappears from the expansion in the end. We assume that z is $O(1)$ and so $\delta \ll 1$ essentially describes the distance from the tip $\xi = 1$. Through this scaling we can explore the dominant behavior of the propagating fracture in a very general way: we have not yet specified the distance from the tip and we do not make a semi-infinite approximation, as used in previous studies such as [6, 26, 24], amongst others.

Because of the symmetry of the solution about $\xi = 0$ (see Figure 1.1), we can restrict our attention to the interval $0 < \xi < 1$ and write the equations in terms of z. The integral in (2.4) is then written as

$$\Pi = -\frac{1}{4\pi\gamma}\int_{-1}^{1} \frac{\mathrm{d}\Omega}{\mathrm{d}\chi}\frac{\mathrm{d}\chi}{\chi - \xi} = -\frac{1}{2\pi\gamma}\int_0^1 \frac{\mathrm{d}\Omega}{\mathrm{d}\chi}\frac{\chi \, \mathrm{d}\chi}{\chi^2 - \xi^2}, \tag{2.9}$$

and similarly for the integrals in (2.6).

Then applying (2.7) and (2.8) in the governing equations (2.3)–(2.6) yields

$$\frac{t(\epsilon L)_t}{\epsilon L}\Omega + (1-\delta z)\frac{t(L\gamma)_t}{L\gamma}\delta^{-1}\frac{\mathrm{d}\Omega}{\mathrm{d}z} + \hat{\mathcal{G}}_c\delta^{\beta_c}\Gamma_l = \frac{1}{\hat{\mathcal{G}}_m\gamma^2}\delta^{-\beta_m-2}\frac{\mathrm{d}}{\mathrm{d}z}\left[\Omega^3\frac{\mathrm{d}\Pi}{\mathrm{d}z}\right], \tag{2.10}$$

$$\Pi = -\frac{1}{2\pi\gamma}\delta^{-1}\int_0^{1/\delta}\frac{\mathrm{d}\Omega}{\mathrm{d}r}\frac{(1-\delta r)}{r(2-\delta r)-z(2-\delta z)}\,\mathrm{d}r, \tag{2.11}$$

$$\Omega = \hat{\mathcal{G}}_k\gamma^{1/2}\delta^{\beta_k+1/2}z^{1/2}, \quad z\longrightarrow 0; \qquad \Omega = 0, \ \ \Omega^3\frac{\mathrm{d}\Pi}{\mathrm{d}z} = 0, \quad \text{at } z=0, \tag{2.12}$$

$$\delta^{\beta_v}\hat{\mathcal{G}}_v = 2\gamma\delta\int_0^{1/\delta}\Omega\,\mathrm{d}r + 2\frac{\hat{\mathcal{G}}_c}{L}\delta^{\beta_c+1}\int_0^1 l(\theta t)\theta^{-1/2}\int_0^{1/\delta}\Gamma_l\,\mathrm{d}r\,\mathrm{d}\theta. \tag{2.13}$$

Here we look for self-similar solutions $\Omega = \Omega(z)$ and $\Pi = \Pi(z)$. We justify the use of these types of solutions in section 3.3. In (2.10)–(2.13) the powers of δ appear explicitly, and they play a central role in understanding the spatial behavior of the solution relative to the key dimensionless quantities.

For $\delta \ll 1$, we expand the solution Ω and Π as follows:

$$\Omega = \delta^{\beta_k+1/2}\big(\Omega_{00} + \delta^{\alpha_1}\Omega_{01} + \delta^{\alpha_2}\Omega_2 + \cdots\big), \tag{2.14}$$

$$\Pi = \delta^{\beta_k}\Pi_{00} + \delta^{\sigma_1}\Pi_{01} + \delta^{\sigma_2}\Pi_2 + \cdots, \tag{2.15}$$

where the exponents α_i and σ_i are determined in terms of the exponents $\beta_{()}$ in (2.8) as part of the method. The prefactor δ^{β_k} corresponds to the dimensionless parameter $\mathcal{G}_k$, and its inclusion in the leading terms is discussed below.

We substitute Ω and Π into the lubrication and elasticity equations (2.10) and (2.11), so that they become, respectively,

$$\begin{aligned}
&\frac{t(\epsilon L)_t}{\epsilon L}\delta^{\beta_k+1/2}\big(\Omega_{00}+\delta^{\alpha_1}\Omega_{01}+\cdots\big)\\
&\quad + (1-\delta z)\frac{t(L\gamma)_t}{L\gamma}\delta^{\beta_k-1/2}\left(\frac{\mathrm{d}\Omega_{00}}{\mathrm{d}z}+\delta^{\alpha_1}\frac{\mathrm{d}\Omega_{01}}{\mathrm{d}z}+\cdots\right) + \hat{\mathcal{G}}_c\delta^{\beta_c}\Gamma_l\\
&\quad = \frac{1}{\hat{\mathcal{G}}_m\gamma^2}\delta^{-\beta_m-1/2+3\beta_k}\frac{\mathrm{d}}{\mathrm{d}z}\left[\big(\Omega_{00}+\delta^{\alpha_1}\Omega_{01}+\big)^3\left(\delta^{\beta_k}\frac{\mathrm{d}\Pi_{00}}{\mathrm{d}z}+\delta^{\sigma_1}\frac{\mathrm{d}\Pi_{01}}{\mathrm{d}z}+\cdots\right)\right],
\end{aligned} \tag{2.16}$$

$$\begin{aligned}
&\delta^{\beta_k}\Pi_{00}+\delta^{\sigma_1}\Pi_{01}+\cdots\\
&\quad = -\frac{1}{2\pi\gamma}\delta^{\beta_k-1/2}\int_0^{1/\delta}\left(\frac{\mathrm{d}\Omega_{00}}{\mathrm{d}r}+\delta^{\alpha_1}\frac{\mathrm{d}\Omega_{01}}{\mathrm{d}r}+\cdots\right)\frac{(1-\delta r)}{r(2-\delta r)-z(2-\delta z)}\,\mathrm{d}r.
\end{aligned} \tag{2.17}$$

The nondimensionalized leak-off function Γ_l is defined as

$$\Gamma_l = \frac{1}{\sqrt{1-t_0(\xi l)/t}} = \frac{1}{\sqrt{1-\xi^{1/\lambda}}} = \frac{1}{\sqrt{1-(1-\delta z)^{1/\lambda}}}, \tag{2.18}$$

where $t_0(\cdot)$ is defined following (1.8), and we have written it in the rescaled coordinates (2.7). This follows from the definition of $t_0(x)$, the time lapsed between the current time t and the time at which the crack tip arrived at the point x, so that $x(t_0(x)) = l(t_0)$. Using $l = \gamma L$, $L = C_L t^\lambda$, and $\xi = x/l$, we find

$$l(t_0) = C_L\gamma\left(\frac{t_0}{t}\right)^\lambda t^\lambda \qquad \text{and} \qquad \frac{t_0}{t} = \xi^{1/\lambda}. \tag{2.19}$$

To motivate the equations which are solved below to leading order in the different regions, we briefly consider the lubrication equation in the form of (2.10). The leading order terms for $\delta \ll 1$ satisfy

$$\lambda\delta^{-1}\frac{\mathrm{d}\Omega}{\mathrm{d}z} + \frac{\hat{\mathcal{G}}_c\delta^{\beta_c-1/2}}{\sqrt{1-(1-\delta z)^{1/\lambda}}} = \frac{1}{\hat{\mathcal{G}}_m\gamma^2}\delta^{-\beta_m-2}\frac{\mathrm{d}}{\mathrm{d}z}\left[\Omega^3\frac{\mathrm{d}\Pi}{\mathrm{d}z}\right]. \tag{2.20}$$

The form of the expansions (2.14) and (2.15) distinguish where toughness dominates, with the sign of α_1 playing a significant role. We consider three cases:

(i) The right-hand side of (2.20) is dominant and set equal to zero. This gives $\Pi = \text{constant}$ to leading order (see Appendix A.1). Then Ω is found using the propagation condition (2.12), giving the leading order square root behavior for Ω_{00} and $\Pi_{00} = \text{constant}$. This case is described by $\alpha_1 > 0$, where toughness dominates the leading order behavior, and thus justifies the use of the prefactor δ^{β_k} in expansions (2.14) and (2.15). The details of this *near-tip* case are given in section 3.1 below.

(ii) The first term on the left-hand side balances with the right-hand side, thus neglecting the term with coefficient $\mathcal{G}_c$ to leading order. This case is described by $\alpha_1 < 0$, where viscosity, not leak-off, dictates the leading order behavior of $z^{2/3}$ [6, 15, 24]. When $\alpha_1 < 0$, the ordering of the terms in (2.14) and (2.15) changes; then Ω_{01} and Π_{01} become leading order and so Ω_{00} and Π_{00} are zero in regions where the toughness is not dominant.

(iii) The second term on the left-hand side matches the right-hand side. We obtain the solution $z^{5/8}$ to leading order, as in [6, 36]. This situation also holds for $\alpha_1 < 0$, with both leak-off and viscosity dictating the leading order behavior. Again, Ω_{00} and Π_{00} are zero, and Ω_{01} and Π_{01} are the leading order terms. The details of this *intermediate-tip* case are given in section 3.1 below. In section 3.3 we show that $\lambda = 1/2$ for sufficiently large time, as in [6], and so we use $\Gamma_l = 1/\sqrt{\delta z(2-\delta z)}$ in (2.18) for this case.

3. The expansion including toughness, leak-off, and viscosity. We consider the case with nonzero leak-off $\mathcal{G}_c \neq 0$ in addition to nonzero toughness and viscosity ($\mathcal{G}_k \neq 0$ and $\mathcal{G}_m \neq 0$.) The expansions (2.14) and (2.15) are used to determine exponents by balancing terms, leading to important combinations of the parameters in (1.11) which characterize the different cases. We focus on scenarios with significant leak-off, leading to the study of transitions between regimes where toughness and leak-off dominate the behavior, namely, cases (i) and (iii). The analysis identifies a critical scaling involving all three processes and gives a parametric characterization for significant leak-off as $\mathcal{G}_c^3/\mathcal{G}_m = O(1)$ or larger. In contrast, case (ii) occurs in regimes where leak-off plays a secondary role, $\mathcal{G}_c^3/\mathcal{G}_m \ll 1$ and $\mathcal{G}_c < \mathcal{G}_k$, and corresponds to the purely viscosity-dominated case with $z^{2/3}$ power law to leading order away from the tip. A straightforward extension of the analysis in [44] of the impermeable case can be used to include higher order corrections involving leak-off in this parameter region, so we do not consider it here. The intermediate case where $\mathcal{G}_c^3/\mathcal{G}_m \ll 1$ and $\mathcal{G}_c < \mathcal{G}_k$ has two transition regions, from the $z^{1/2}$ to $z^{5/8}$ to $z^{2/3}$ behavior. The analyses presented below and in [44] can be extended easily to treat these two transitions, and we outline this situation in section 4.

3.1. Local expansions. *Near-tip behavior* ($\alpha_1 > 0$): The leading order terms in (2.16) and (2.17) for $\delta \ll 1$ satisfy

$$0 = \delta^{-\beta_m - 1/2 + 4\beta_k} \frac{\mathrm{d}}{\mathrm{d}z}\left[\Omega_{00}^3 \frac{\mathrm{d}\Pi_{00}}{\mathrm{d}z}\right], \tag{3.1}$$

$$\delta^{\beta_k}\Pi_{00} = -\frac{1}{2\pi\gamma}\delta^{\beta_k - 1/2}\int_0^{1/\delta} \frac{\mathrm{d}\Omega_{00}}{\mathrm{d}r}\frac{(1-\delta r)}{r(2-\delta r) - z(2-\delta z)}\,\mathrm{d}r. \tag{3.2}$$

From these two equations we deduce that the solution of Ω_{00} is

$$\Omega_{00}(z) = C_{00}\sqrt{z(2-\delta z)}, \tag{3.3}$$

where $C_{00} = 4\pi\Pi_{00}$, and $\Pi_{00} =$ constant, as discussed in Appendix A.1. The expression (3.3) is the eigenfunction solution which, when substituted into (3.2), gives $\Pi_{00} =$ constant exactly; its leading order behavior matches the tip condition (2.12) and it is symmetric about $\xi = 0$. We use the tip condition (2.12) to find $C_{00} = \hat{\mathcal{G}}_k\sqrt{\gamma/2}$. Note that for $\alpha_1 > 0$, the leading order term in the expansion for Ω involves the rescaled toughness parameter $\mathcal{G}_k$.

The next order terms for $\delta \ll 1$ in (2.16) and (2.17) satisfy

$$\lambda\delta^{\beta_k - 1/2}\frac{\mathrm{d}\Omega_{00}}{\mathrm{d}z} + \hat{\mathcal{G}}_c\sqrt{\lambda}\delta^{\beta_c - 1/2}z^{-1/2} = \frac{1}{\hat{\mathcal{G}}_m\gamma^2}\delta^{-\beta_m + 3\beta_k - 1/2 + \sigma_1}\frac{\mathrm{d}}{\mathrm{d}z}\left[\Omega_{00}^3\frac{\mathrm{d}\Pi_{01}}{\mathrm{d}z}\right], \tag{3.4}$$

$$\delta^{\sigma_1}\Pi_{01} = -\frac{1}{2\pi\gamma}\delta^{\beta_k - 1/2 + \alpha_1}\int_0^{1/\delta}\frac{\mathrm{d}\Omega_{01}}{\mathrm{d}r}\frac{(1-\delta r)}{r(2-\delta r) - z(2-\delta z)}\,\mathrm{d}r. \tag{3.5}$$

For the moment we do not balance exponents of δ, but leave them in the expression. Solving (3.4) and (3.5) gives Ω_{01} and Π_{01}: we find $\Omega_{01}(z) = C_{01}z$ and Π_{01} satisfies

$$\Pi_{01} = -\frac{C_{01}}{4\pi\gamma}\ln\left(1 - \frac{1}{2-\delta z}\right) - \frac{C_{01}}{4\pi\gamma}\left[\ln(1-\delta z) - \ln(\delta z)\right] \tag{3.6}$$

for $z = O(1)$. The constant of integration in (3.4) is zero; otherwise the solution for Π_{01} yields an infinite stress intensity factor, as shown in Appendix A.2. The details of the calculation of Π_{01} are similar to the analysis in Appendix B. We now determine C_{01} by substituting Π_{01} into (3.4), and considering the leading order terms only. Hence

$$\delta^{\sigma_1}C_{01} = \hat{\mathcal{G}}_m\gamma^2\left[\delta^{\beta_m - 2\beta_k}\lambda\frac{2\pi\gamma}{C_{00}^2} + \delta^{\beta_c + \beta_m - 3\beta_k}\frac{4\pi\gamma\sqrt{\lambda}\hat{\mathcal{G}}_c}{\sqrt{2}C_{00}^3}\right]. \tag{3.7}$$

Notice that the terms on the right-hand side of (3.7) change order depending on the relative magnitude of $\mathcal{G}_k$ and $\mathcal{G}_c$ (i.e., δ^{β_k} and δ^{β_c}.) If $\mathcal{G}_c \ll \mathcal{G}_k$, then the first term on the right-hand side is dominant and we obtain

$$\alpha_1 = 1/2 + \beta_m - 3\beta_k, \qquad \sigma_1 = \beta_m - 2\beta_k, \qquad C_{01} = 2\pi\lambda\frac{\hat{\mathcal{G}}_m\gamma^3}{C_{00}^2}. \tag{3.8}$$

However, if $\mathcal{G}_c \gg \mathcal{G}_k$, then the second term on the right-hand side of (3.7) is dominant. The exponents α_1 and σ_1 and coefficient C_{01} are now

$$\alpha_1 = 1/2 + \beta_c + \beta_m - 4\beta_k, \qquad \sigma_1 = \beta_c + \beta_m - 3\beta_k, \qquad C_{01} = \frac{4\pi\sqrt{\lambda}\hat{\mathcal{G}}_c\hat{\mathcal{G}}_m\gamma^3}{\sqrt{2}C_{00}^3}. \tag{3.9}$$

Since both of these cases represent particular solutions to the linear equations (3.4)–(3.5), we can treat them simultaneously. Thus if $\alpha_1 > 0$, the first three terms in the expansion (2.14) for Ω are

$$\Omega \sim \delta^{\beta_k+1/2}\left[C_{00}\sqrt{z(2-\delta z)} + \delta^{1/2+\beta_m-3\beta_k}C_{01}z + \delta^{1/2+\beta_c+\beta_m-4\beta_k}C_{02}z\right], \tag{3.10}$$

where C_{02} is the redefined C_{01} coefficient from (3.9). Then the second term dominates over the third term when $\mathcal{G}_c \ll \mathcal{G}_k$, and vice versa when $\mathcal{G}_c \gg \mathcal{G}_k$.

Intermediate-tip behavior ($\alpha_1 < 0$): The leading order terms in (2.16) are

$$\lambda\delta^{\beta_k-1/2+\alpha_1}\frac{\mathrm{d}\Omega_{01}}{\mathrm{d}z} + \frac{\hat{\mathcal{G}}_c\delta^{\beta_c-1/2}}{\sqrt{z(2-\delta z)}} = \frac{\delta^{-\beta_m+3\beta_k-1/2+3\alpha_1+\sigma_1}}{\hat{\mathcal{G}}_m\gamma^2}\frac{\mathrm{d}}{\mathrm{d}z}\left[\Omega_{01}^3\frac{\mathrm{d}\Pi_{01}}{\mathrm{d}z}\right], \tag{3.11}$$

coupled with the elasticity equation (3.5). Note that we now use the form of Γ_l with $\lambda = 1/2$, as mentioned in case (iii) above, since we are in the leak-off–dominated regime. In the case that $\mathcal{G}_c^3/\mathcal{G}_m \gg (1-\xi)^{1/2}$, the second term on the left-hand side of (3.11) is dominant over the term with $\Omega_{01}'(z)$. Then balancing powers of δ in (3.11) and the elasticity equation (3.5) gives

$$\alpha_1 = 1/8 + (\beta_c+\beta_m)/4 - \beta_k, \qquad \sigma_1 = -3/8 + (\beta_c+\beta_m)/4. \tag{3.12}$$

Note that if the first term in (3.11) is dominant, then the leading order terms for Ω_{01} are the same as in the case of zero leak-off studied in [6, 15, 24, 44]. This corresponds to the case $\delta^{1/8+(\beta_m+\beta_c)/4} > \delta^{\beta_c}$ or, equivalently, $\mathcal{G}_c^3/\mathcal{G}_m \ll (1-\xi)^{1/2}$. Ignoring this term to leading order is consistent with the fact that leak-off is dominant, i.e., $\mathcal{G}_c^3/\mathcal{G}_m = O(1)$ or larger, as discussed in section 3.

The form of Ω_{01} is written as a combination of powers in z, namely,

$$\Omega_{01} = \tilde{C}_{01}z^q + \hat{\mathcal{B}}_1 z^g + \hat{\mathcal{B}}_2 z^p + \hat{\mathcal{B}}_3 z^r. \tag{3.13}$$

This is equivalent to a perturbation expansion for the solution of (3.11) when $\hat{\mathcal{B}}_i \ll 1$, which we verify below. The elasticity equation (3.5) is then solved to give

$$\begin{aligned}\Pi_{01} = {} & \cot\pi q\frac{\tilde{C}_{01}q}{4\gamma}z^{q-1} + \cot\pi g\frac{\hat{\mathcal{B}}_1 g}{4\gamma}z^{g-1} + \cot\pi p\frac{\hat{\mathcal{B}}_2 p}{4\gamma}z^{p-1} + \cot\pi r\frac{\hat{\mathcal{B}}_3 r}{4\gamma}z^{r-1} \\ & + \frac{\tilde{C}_{01}q\delta^{1-q}(2-\delta z)^{-1}}{4\pi\gamma} + \frac{\hat{\mathcal{B}}_1 g\delta^{1-g}(2-\delta z)^{-1}}{4\pi\gamma} + \frac{\hat{\mathcal{B}}_2 p\delta^{1-p}(2-\delta z)^{-1}}{4\pi\gamma} \\ & + \frac{\hat{\mathcal{B}}_3 r\delta^{1-r}(2-\delta z)^{-1}}{4\pi\gamma} + O(\delta^{1-q},\delta^{1-g},\delta^{1-p},\delta^{1-r}).\end{aligned} \tag{3.14}$$

By using the definitions of α_1 and σ_1 from (3.12) we integrate (3.11) to obtain

$$\lambda\delta^{1/8+\beta_m/4-3\beta_c/4}\Omega_{01} + \hat{\mathcal{G}}_c\sqrt{2}\left(z^{1/2} + \frac{1}{12}\delta z^{3/2}\right) + k = \frac{1}{\hat{\mathcal{G}}_m\gamma^2}\Omega_{01}^3\frac{\mathrm{d}\Pi_{01}}{\mathrm{d}z}, \tag{3.15}$$

where k is an arbitrary constant. We then have four expressions enabling us to determine q, g, p, and r. The leading order terms are

$$\sqrt{2}\hat{\mathcal{G}}_c z^{1/2} = \cot\pi q\frac{\tilde{C}_{01}^4 q(q-1)}{4\hat{\mathcal{G}}_m\gamma^3}z^{4q-2}, \tag{3.16}$$

which yields $q = 5/8$ and gives the coefficient $\tilde{C}_{01}$,

$$\tilde{C}_{01} = \left\{ \frac{4\sqrt{2}\hat{\mathcal{G}}_c\hat{\mathcal{G}}_m\gamma^3}{q(q-1)\cot\pi q} \right\}^{1/4}. \tag{3.17}$$

Then the next order terms satisfy

$$k = \frac{\tilde{C}_{01}^3\hat{\mathcal{B}}_1}{4\hat{\mathcal{G}}_m\gamma^3}\big[g(g-1)\cot\pi g + 3q(q-1)\cot\pi q\big] z^{3q+g-2}, \tag{3.18}$$

$$\lambda\delta^{1/8+(\beta_m-3\beta_c)/4}\tilde{C}_{01}z^q = \frac{\tilde{C}_{01}^3\hat{\mathcal{B}}_2}{4\hat{\mathcal{G}}_m\gamma^3}\big[p(p-1)\cot\pi p + 3q(q-1)\cot\pi q\big] z^{3q+p-2}, \tag{3.19}$$

$$\lambda\delta^{1/8+(\beta_m-3\beta_c)/4}\hat{\mathcal{B}}_1z^g = \frac{\tilde{C}_{01}^3\hat{\mathcal{B}}_3}{4\hat{\mathcal{G}}_m\gamma^3}\big[r(r-1)\cot\pi r + 3q(q-1)\cot\pi q\big] z^{3q+r-2}. \tag{3.20}$$

For simplicity of presentation we assume $\delta^{1/8+(\beta_m-3\beta_c)/4} > \delta$, which means we can neglect the $z^{3/2}$ term in (3.15). This corresponds to the case $\mathcal{G}_c^3/\mathcal{G}_m \ll (1-\xi)^{-7/2}$. Including this term results in an additional contribution to Ω_{01} in (3.13) with power law $z^{13/8}$. This term can be shown to be higher order in the matching below and could be included in a straightforward manner if $\mathcal{G}_c^3/\mathcal{G}_m = O((1-\xi)^{-7/2})$ or larger.

Matching exponents of z in (3.18)–(3.19) gives $g = 1/8$ and $p = 3/4$, respectively. Since $\hat{\mathcal{B}}_1$ is assumed small, the left-hand side of (3.20) is of higher order; r must be approximated by solving the following nonlinear algebraic equation corresponding to the right-hand side of (3.20) vanishing:

$$r(r-1)\cot\pi r + 3q(q-1)\cot\pi q = 0, \tag{3.21}$$

and we find that $r \approx 0.0699928$. Then

$$\hat{\mathcal{B}}_2 = \delta^{1/8+(\beta_m-3\beta_c)/4}\mathcal{B}_2, \qquad \mathcal{B}_2 = \lambda\frac{4\hat{\mathcal{G}}_m\gamma^3}{\tilde{C}_{01}^2\big[p(p-1)cot\pi p + 3q(q-1)cot\pi q\big]}, \tag{3.22}$$

and the coefficients $\hat{\mathcal{B}}_1$ and $\hat{\mathcal{B}}_3$ are determined by matching with the near-tip expansion (3.10) in the next section. Since $q,\ g,\ p,\ r \neq 1/2$, the solution (3.13) cannot satisfy the $\sqrt{z}$ behavior from the propagation condition (2.12) for $\hat{\mathcal{G}}_k > 0$. Observe that for $\alpha_1 < 0$, toughness does not dominate the leading order behavior in this regime and the terms $\Omega_{00} = \Pi_{00} = 0$. Then the first term in the expansion (2.14) for Ω is

$$\Omega \sim \delta^{(\beta_c+\beta_m)/4}\left[\tilde{C}_{01}(\delta z)^{5/8} + \mathcal{B}_1(\delta z)^{1/8} + \mathcal{B}_2\delta^{(\beta_m-3\beta_c)/4}\frac{\hat{\mathcal{G}}_m^{1/4}}{\hat{\mathcal{G}}_c^{3/4}}(\delta z)^{3/4} + \mathcal{B}_3(\delta z)^r\right] \tag{3.23}$$

for $\alpha_1 < 0$. Note that we have redefined $\tilde{C}_{01}$ and $\mathcal{B}_2$ without the $\hat{\mathcal{G}}_()$ terms, which allows us to highlight explicitly the dependence of Ω on the key dimensionless quantities $\mathcal{G}_()$ in (2.2). The coefficients $\hat{\mathcal{B}}_1$ and $\hat{\mathcal{B}}_3$ are redefined as $\mathcal{B}_1$ and $\mathcal{B}_3$ and they are found in the following section.

3.2. Transition in spatial behavior and matching. Now we compare the two local expansions, (3.10) and (3.23), in terms of the parameter combinations

$$\mathcal{P}_{km} = \frac{\mathcal{G}_k^3}{\mathcal{G}_m}, \qquad \mathcal{P}_{cm} = \frac{\mathcal{G}_c^3}{\mathcal{G}_m}, \qquad \mathcal{P}_{ckm} = \frac{\mathcal{G}_k^4}{\mathcal{G}_c\mathcal{G}_m}, \tag{3.24}$$

which appear explicitly in both expansions and were introduced in (1.11). We consider the range of parameters for which either $\mathcal{P}_{cm} \gg (1-\xi)^{1/2}$ or $\mathcal{P}_{km} \gg (1-\xi)^{1/2}$, i.e., parameter values away from the viscosity-dominated regime. For $\mathcal{G}_c = O(1)$ this corresponds to $\mathcal{G}_m \ll 1$ or $\beta_m > 1$. Other situations are discussed in the next section.

Then the expansions for Ω in terms of $\mathcal{P}_{km}$, $\mathcal{P}_{cm}$, and $\mathcal{P}_{ckm}$ are

$$\Omega \sim \mathcal{G}_k \left[C_{00}\sqrt{1-\xi^2} + C_{01}\mathcal{P}_{km}^{-1}(1-\xi) + C_{02}\mathcal{P}_{ckm}^{-1}(1-\xi) \right] \quad \text{for } \alpha_1 > 0, \tag{3.25}$$

$$\Omega \sim (\mathcal{G}_c\mathcal{G}_m)^{1/4} \left[\tilde{C}_{01}(1-\xi)^{5/8} + \mathcal{B}_1(\mathcal{P}_{ckm})(1-\xi)^{1/8} + \mathcal{P}_{cm}^{-1/4}\mathcal{B}_2(1-\xi)^{3/4} + \mathcal{B}_3(\mathcal{P}_{ckm})(1-\xi)^{r} \right] \quad \text{for } \alpha_1 < 0. \tag{3.26}$$

We have redefined C_{00}, C_{01}, and C_{02} in (3.25) without the $\hat{\mathcal{G}}_{()}$ terms which are incorporated into the dimensionless $\mathcal{G}_{()}$ terms. Also, observe that the δ's have disappeared from the expressions. The expansions (3.25)–(3.26) give a transition in behavior of Ω for $1-\xi = O(\mathcal{P}_{ckm}^2)$: the unknown coefficients $\mathcal{B}_1(\mathcal{P}_{ckm})$ and $\mathcal{B}_3(\mathcal{P}_{ckm})$ are determined by matching the expansions in this transition region. The leading order term in (3.26) was given in [36] and later in [6] for vanishing toughness. In a preliminary study [9] some of the terms in (3.26) are obtained. There, both the global balance and lubrication equations are scaled by ${\mathcal{G}_v}^{-1}$, and they consider the limit of small toughness, with $\mathcal{G}_v \to \infty$, for fixed nondimensional parameters $\mathcal{G}_c/\mathcal{G}_v = \mathcal{G}_m\mathcal{G}_v = 1$. Then some of the terms in (3.26) are excluded for large $\mathcal{G}_v$.

The motivation for defining the parameter $\mathcal{P}_{ckm}$ follows directly from the expression for α_1 in both cases, i.e., (3.9) and (3.12). Since the $\hat{\mathcal{G}}_{()}$ quantities are $O(1)$, the condition $\alpha_1 > (<)\, 0$ can be rewritten as $\mathcal{P}_{ckm} \gg (\ll)\,(1-\xi)^{1/2}$. The solution for $\alpha_1 > 0$ is physically significant in the toughness dominated regime ($\mathcal{G}_k \gg \mathcal{G}_c$), which is close to the tip and corresponds to $\mathcal{P}_{ckm} \gg (1-\xi)^{1/2}$. As $(1-\xi)^{7/2}$ approaches $\mathcal{P}_{ckm}$, the first and third terms in (3.25) and the first term in (3.26) are the same order of magnitude. A transition occurs in the region $(1-\xi) = O(\mathcal{P}_{ckm}^{1/2})$ and the solution in the intermediate-tip region is found by considering $\alpha_1 < 0$ in (3.26). This corresponds to the leak-off dominated regime, which is away from the tip for $\mathcal{P}_{ckm} \ll (1-\xi)^{1/2}$. Hence the expansion in (3.25) holds for $1-\xi < \mathcal{P}_{ckm}^2$ and the expansion in (3.26) holds for $1-\xi = O(\mathcal{P}_{ckm}^s)$ (see Figure 3.1), with $0 < s < 2$, and $\mathcal{P}_{ckm} \ll 1$.

To construct a uniform asymptotic approximation by matching (3.25) and (3.26), we note that they are obtained by solving (2.20) in different asymptotic limits. The matching is therefore straightforward in the transition region where $\mathcal{G}_k^4/(\mathcal{G}_c\mathcal{G}_m) = O((1-\xi)^{1/2})$; to leading order the solution satisfies (2.20) together with the propagation condition (2.12). While there is no closed form solution in this region, it can be constructed numerically where $1-\xi = O(\mathcal{P}_{ckm}^2)$ for $0 < \mathcal{P}_{ckm} \ll 1$.

Alternatively, one can give an analytical expression for the matching of (3.25) and (3.26), obtained from solving for the remaining unknown coefficients $\mathcal{B}_1(\mathcal{P}_{ckm})$ and $\mathcal{B}_3(\mathcal{P}_{ckm})$. Writing these expressions in terms of the critical scaling $1-\xi = \mathcal{P}_{ckm}^2\zeta$ for $\zeta = 0(1)$, (3.25) and (3.26) are, respectively,

$$\Omega \sim \mathcal{G}_k \left[C_{00}\mathcal{P}_{ckm}\zeta^{1/2}\sqrt{2-\mathcal{P}_{ckm}^2\zeta} + \left(C_{01}\mathcal{P}_{km}^{-1} + C_{02}\mathcal{P}_{ckm}^{-1}\right)\mathcal{P}_{ckm}^2\zeta \right], \tag{3.27}$$

$$\Omega \sim (\mathcal{G}_c\mathcal{G}_m)^{1/4} \left[\tilde{C}_{01}\mathcal{P}_{ckm}^{5/4}\zeta^{5/8} + \mathcal{B}_1(\mathcal{P}_{ckm})\mathcal{P}_{ckm}^{1/4}\zeta^{1/8} + \mathcal{P}_{cm}^{-1/4}\mathcal{B}_2\mathcal{P}_{ckm}^{3/2}\zeta^{3/4} + \mathcal{B}_3(\mathcal{P}_{ckm})\mathcal{P}_{ckm}^{2r}\zeta^{r} \right]. \tag{3.28}$$

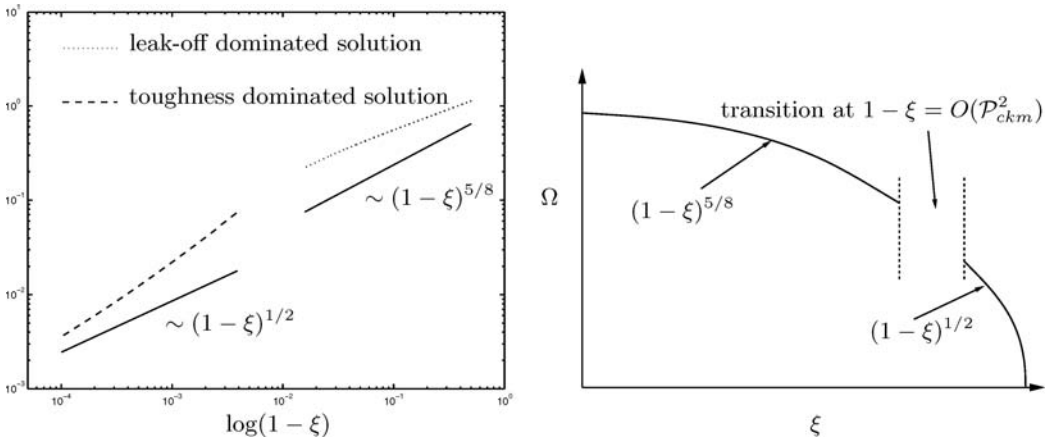

FIG. 3.1. *The left plot shows* $\log\Omega$ *vs.* $\log(1-\xi)$ *with* $\mathcal{G}_c = 1$, $\mathcal{G}_m = 0.2$, *and* $\mathcal{G}_k = 0.35$ *(and so* $\mathcal{P}_{ckm} = 0.075$*.) The solid lines denote the leading order power law solutions, as indicated above. The right plot shows a diagram of the solution* Ω *vs.* ξ *near the fracture tip for the leak-off–dominated regime. The transition region is* $1-\xi = O(\mathcal{P}_{ckm}^2)$.

Equating (3.27) and (3.28) and their first derivatives yields $\mathcal{B}_1(\mathcal{P}_{ckm})$ and $\mathcal{B}_3(\mathcal{P}_{ckm})$, which is equivalent to matching the first two terms in a Taylor series expansion about $1-\xi = O(\mathcal{P}_{ckm}^2)$ where Ω is regular. Figure 3.2 shows solution profiles of Ω, matched at $1-\xi = \mathcal{P}_{ckm}^2$. In these parameter regimes all three processes contribute to the transition between the near- and intermediate-tip behavior, described by (3.25) and (3.26). There the coefficients $\mathcal{B}_1(\mathcal{P}_{ckm})$ and $\mathcal{B}_3(\mathcal{P}_{ckm})$ are

$$\mathcal{B}_1(\mathcal{P}_{ckm}) = \frac{\mathcal{P}_{ckm}}{8r-1}\Big[(8r-4)\sqrt{2}C_{00} + (8r-8)\big(C_{01}\mathcal{P}_{km}^{-1}\mathcal{P}_{ckm} + C_{02}\big) - (8r-5)\tilde{C}_{01} - (8r-6)\mathcal{B}_2\mathcal{P}_{cm}^{-1/4}\mathcal{P}_{ckm}^{1/4}\Big], \tag{3.29}$$

$$\mathcal{B}_3(\mathcal{P}_{ckm}) = \frac{\mathcal{P}_{ckm}^{-2r+5/4}}{8r-1}\Big[3\sqrt{2}C_{00} + 7C_{01}\mathcal{P}_{km}^{-1}\mathcal{P}_{ckm} + 7C_{02} - 4\tilde{C}_{01} - 5\mathcal{B}_2\mathcal{P}_{cm}^{-1/4}\mathcal{P}_{ckm}^{1/4}\Big], \tag{3.30}$$

which are small since $\mathcal{P}_{ckm} \ll 1$. As $\mathcal{P}_{ckm}$ increases we observe that the transition region moves away from the tip. Figure 3.2 also shows two solution profiles when (3.25) holds to leading order for both near- and intermediate-tip behavior for $\mathcal{P}_{ckm} < \mathcal{P}_{km}$ and $\mathcal{P}_{ckm} > \mathcal{P}_{km}$. The shape of Ω depends on whether the second or third term in (3.25) plays a larger role in the correction to the leading order behavior. Also, Figure 3.1 shows a log-log plot of Ω for both the leak-off and toughness-dominated regimes. In the near- and intermediate-tip regions we obtain the asymptotic 1/2 and 5/8 power law solutions, respectively, but in the transition region the correction terms are important, so that the behavior cannot be described by a purely power law solution, also observed in [6, 24] for zero leak-off.

For completeness we write down the near- and intermediate-tip expansions for Π, which are determined using the elasticity equation (2.11). Hence we obtain, for

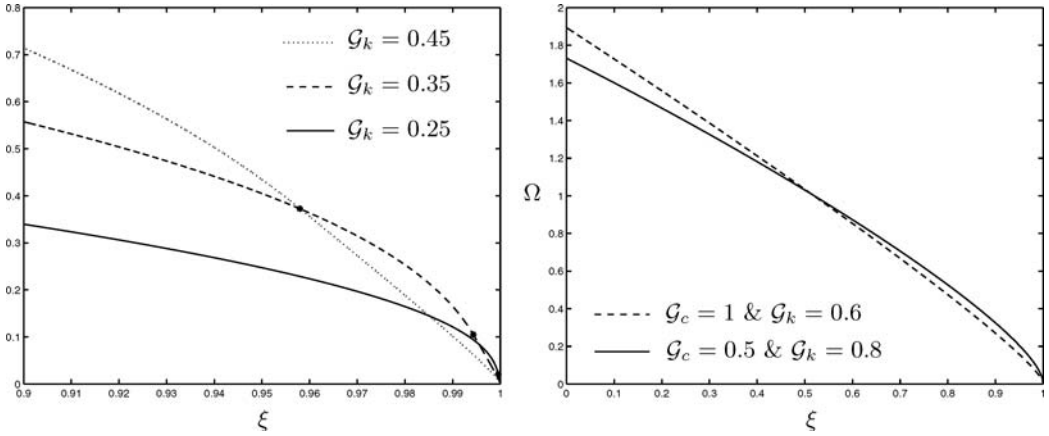

FIG. 3.2. *Solution profiles of* Ω *vs.* ξ. *On the left,* $\mathcal{G}_c = 1$, $\mathcal{G}_m = 0.2$, *and* $\mathcal{G}_k = 0.45, 0.35, 0.25$ *(and* $\mathcal{P}_{ckm} = 0.205, 0.075, 0.020$, *respectively). The transition region is* $1 - \xi = O(\mathcal{P}_{ckm}^2)$, *indicated by* $*$*'s at* $\xi = 1 - \mathcal{P}_{ckm}^2$ *on the graphs. On the right,* $\mathcal{G}_m = 0.1$; *then, for the toughness dominated regime (solid line),* $\mathcal{P}_{ckm} = 8.192$ *and* $\mathcal{P}_{km} = 5.12$, *and for the leak-off dominated regime (dashed line),* $\mathcal{P}_{ckm} = 1.296$ *and* $\mathcal{P}_{km} = 2.16$.

$\mathcal{P}_{ckm} \gg (\ll) (1-\xi)^{1/2}$, respectively,

$$\Pi \sim \mathcal{G}_k \left[\Pi_{00} - \frac{1}{4\pi\gamma} \left(C_{01} \mathcal{P}_{km}^{-1} + C_{02} \mathcal{P}_{ckm}^{-1} \right) \left\{ \ln \left| 1 - \frac{1}{1+\xi} \right| + \ln \left| \frac{1}{1-\xi} \right| + \ln \xi \right\} \right], \tag{3.31}$$

$$\Pi \sim (\mathcal{G}_c \mathcal{G}_m)^{1/4} \left[q \cot \pi q \frac{\tilde{C}_{01}}{4\gamma} (1-\xi)^{-3/8} + g \cot \pi g \frac{\mathcal{B}_1(\mathcal{P}_{ckm})}{4\gamma} (1-\xi)^{-7/8} \right.$$

$$\left. + p \cot \pi p \frac{\mathcal{P}_{cm}^{-1/4} \mathcal{B}_2}{4\gamma} (1-\xi)^{-1/4} + r \cot \pi r \frac{\mathcal{B}_3(\mathcal{P}_{ckm})}{4\gamma} (1-\xi)^{r-1} \right]. \tag{3.32}$$

The details of this calculation are given in Appendix B. In Figure 3.3 we graph Π for different values of $\mathcal{G}_k \ll 1$ with $\mathcal{G}_m = 0.2$ and $\mathcal{G}_c = 1$. We observe that as $\mathcal{P}_{ckm}$ increases, which in this case corresponds to increasing the toughness parameter $\mathcal{G}_k$ since $\mathcal{G}_m$ and $\mathcal{G}_c$ are fixed, the transition point between the two regimes moves away from the tip and Π drops off at a faster rate. This is due to the power law behavior in (3.32) being matched with the near-tip behavior in (3.31), which becomes more dominant through the logarithmic correction for increasing $\mathcal{G}_k$.

3.3. The global volume balance condition. The constants (i.e., the coefficients C_{00}, C_{01}, C_{02}, $\tilde{C}_{01}$, and γ) are determined by applying the global volume balance condition (2.13) and balancing terms according to the size of the parameters. This condition also checks the consistency of the expansion and shows when we need to consider additional time-dependencies which we discuss below.

The global volume balance equation in terms of the ξ scaling is given by (2.6). Since $l = \gamma L$ and $L = C_L t^{\lambda}$, where C_L is an undetermined constant, we use Γ_l defined in (2.18) to simplify the double integral. Hence (2.6) reduces to

$$\mathcal{G}_v = 2\gamma \int_0^1 \Omega \, \mathrm{d}\chi + \frac{2\lambda\sqrt{\pi}\gamma\Gamma(\lambda)\mathcal{G}_c}{(\lambda + 1/2)\Gamma(\lambda + 1/2)}, \tag{3.33}$$

where $\Gamma(\cdot)$ represents the Gamma function. We must analyze the different situations that arise for $\mathcal{P}_{ckm} \gg 1$ and $\mathcal{P}_{ckm} \ll 1$. The former case corresponds to toughness

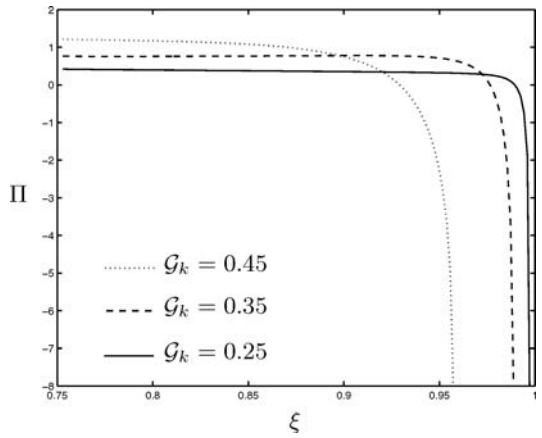

FIG. 3.3. *Solution profiles of* Π *against* ξ *with fixed* $\mathcal{G}_c = 1$, $\mathcal{G}_m = 0.2$, *and* $\mathcal{G}_k = 0.45, 0.35, 0.25$ *(and* $\mathcal{P}_{ckm} = 0.205, 0.075, 0.020$, *respectively).*

dominating the behavior over the whole fracture, with $\alpha_1 > 0$, and is discussed in detail in [44]. Then the left-hand side balances with the integral on the right-hand side to leading order; it follows that $\lambda = 2/3$, that is, $L = C_L t^{2/3}$. Substitution of (3.25) then leads to an expression for γ in terms of $\mathcal{G}_v$ and $\mathcal{G}_k$. The integral is evaluated using the asymptotic expansion near the tip and using numerical evaluation away from the tip where the behavior is regular [6, 24].

In contrast, for the case of $\mathcal{P}_{ckm} \ll 1$, the expansion (3.26) with $\alpha_1 < 0$ must be used for $\mathcal{G}_k^4/(\mathcal{G}_c\mathcal{G}_m) < (1-\xi)^{1/2}$. For this range of ξ the leading order terms in the lubrication equation are those with coefficients $\mathcal{G}_c$ and $\mathcal{G}_m^{-1}$. Together with the elasticity equation, these terms indicate that Ω and Π must scale with $(\mathcal{G}_c\mathcal{G}_m)^{1/4}$, as in (3.26). Then the global balance condition has the form

$$\mathcal{G}_v/\mathcal{G}_c = \text{const} \cdot \mathcal{P}_{cm}^{-1/4} + \text{const}. \tag{3.34}$$

As discussed in section 3.1 following (3.11), $\mathcal{P}_{cm} \gg 1$ in this case, and so the leading order terms are the first and third, and the contribution from the integral is higher order. Then we equate the leading order terms to obtain γ analytically. The global balance equation verifies that the self-similar solution is appropriate for sufficiently large $\mathcal{P}_{cm}$. Writing the t dependence explicitly in (3.34) and using the definitions in (2.2) with $L = C_L t^\lambda$ gives

$$\frac{Q_0}{\epsilon C_L^2} t^{1-2\lambda} = \text{const} \cdot \left(\frac{C'\mu'}{\epsilon^4 C_L E'}\right)^{1/4} t^{-(2\lambda+1)/8} + \text{const} \cdot \frac{C'}{\epsilon C_L} t^{1/2-\lambda}. \tag{3.35}$$

Comparing exponents and balancing the first and third terms gives $\lambda = 1/2$ and the expression for γ simplifies to $\gamma = \mathcal{G}_v/\pi\mathcal{G}_c$. Balancing the first and second terms leads to a contradiction unless $t < 1$. The second term in (3.35) can be neglected for $t^{-1/4} \ll 1$, corresponding to $\mathcal{P}_{cm}^{-1/4} \ll 1$ as in (3.34). This verifies that it is appropriate to use $\lambda = 1/2$ for the leak-off–dominated intermediate-tip behavior in section 3.1 for sufficiently large t. If this condition is violated, for example, for short times, we can no longer conclude that γ is constant, and additional time-dependence must be included in the expansion.

4. Discussion and future work. In conclusion, we have introduced a new approach for studying the system of integrodifferential equations that are found in hydraulic fracturing problems. Our method enables us to simultaneously consider the three primary physical mechanisms, namely, viscosity, toughness, and leak-off, and we have obtained a continuous solution for the fracture opening w when one or more of these processes are in balance. The technique determines critical relationships between the nondimensional distance from the tip $1-\xi$ and the key nondimensional quantities $\mathcal{G}_k$, $\mathcal{G}_c$, $\mathcal{G}_m$, and $\mathcal{G}_v$, representing toughness, leak-off, viscosity, and injected fluid volume, respectively.

For small toughness and $O(1)$ leak-off, the behavior of Ω follows from combining (3.25) for values of ξ in the near-tip region, and (3.26) for ξ in the intermediate-tip region. The critical parameter combination in this case is $\mathcal{P}_{ckm} = \mathcal{G}_k^4/\mathcal{G}_c\mathcal{G}_m$, with the transition layer occurring for values of $\mathcal{P}_{ckm} = O((1-\xi)^{1/2})$. Additional higher order corrections depend on the relative magnitude of extra parameter combinations, $\mathcal{P}_{km}$ and $\mathcal{G}_c^3/\mathcal{G}_m = \mathcal{P}_{cm}$. These results are obtained by simultaneously solving the elasticity and lubrication equations (2.10)–(2.11). The physical process of leak-off has often been ignored in previous studies, and the new terms in expansions (3.25) and (3.26) allow us to match expansions in different regions analytically, in contrast to previous work [24] for zero leak-off. This analysis is new and the flexibility is invaluable in extending the technique to other fracture geometries, namely, the PKN fracture [43], and adding different effects, such as stress-jumps and fluid lag. It is important to determine analytic solutions such as those derived in this paper, which can be used to test the validity of the model against more complete numerical models as well as data from laboratory and field experiments.

The application of the global volume balance equation is used to determine the remaining constants in the solution, and it also provides valuable information related to time dependence. In the regimes considered in this paper, we find that it provides a consistency check for the use of a self-similar solution (2.14)–(2.15) with the coefficient γ constant to leading order. We also determine the time-dependence of L, which gives the power law scaling in time of the length of the fracture.

The global volume balance equation can also be used to determine regimes where additional time-dependence must be included in the solution. For example, using this equation, for finite leak-off we can deduce that for large but finite time the coefficient γ varies on a slow time scale, $T = \mathcal{P}_{cm}^{-1/4}t$ for $\mathcal{P}_{cm} \gg 1$. For small time this analysis is not sufficient: then a multiple-scale analysis of the resulting equations is necessary to describe additional time dependence and transient behavior.

As noted in section 1.1 of the introduction, the results presented here rely on the use of Carter's leak-off model (1.8). However, our framework does not depend on a specific form for the leak-off term, so its implementation is not restricted to the use of (1.8). These results are valid for the balance of physical processes corresponding to $O(1)$ (or smaller) leak-off, which is typical of many fracturing treatments due to the cake-building properties of the fracturing fluid [51]. Specifically, we require that the combined parameter $\mathcal{P}_{cm} := \mathcal{G}_c^3/\mathcal{G}_m \gg 1$. In situations where $\mathcal{G}_c \gg 1$, such as in waterflood fractures, the leak-off term is not a higher order correction at the tip, and therefore it would require a different modeling approach in that region.

Typical values of Carter's leak-off coefficient C' range from 4–64×10^{-5} m/s$^{-1/2}$, as discussed in [6] and the references therein. Suppose we consider the case $\mathcal{P}_{ckm} \ll 1$ and set $\mathcal{G}_v = \mathcal{G}_c = 1$. Then the expression for γ, as found in section 3.3, is simply $\gamma = 1/\pi$. Typical values of the other parameters are found in [6, 19, 27]: $Q_0 = 4$–40×10^{-4} m^2/s, $E = 10000$–25000 MPa, $\nu = 0.15$, $\mu = 1 \times 10^{-7}$ MPa$\cdot$s, and

$K_{Ic} = 1$ MPa $\cdot$ m$^{1/2}$. For example, using $Q_0 = 4 \times 10^{-4}$ m^2/s, $C' = 16 \times 10^{-5}$, and $E = 10000$ MPa, the combined parameters can be shown to satisfy $\mathcal{P}_{cm} \approx 0.0022t$, $\mathcal{P}_{ckm} \approx 0.20$, and $\mathcal{P}_{km} \approx 0.066t^{1/4}$. Then the transition region is at $\xi = O(1-\mathcal{P}_{ckm}^2) \approx 0.96$, which supports the values used in the figures in section 3. This also shows that our analysis is applicable for large time, since we require $\mathcal{P}_{cm} \gg 1$. If we increase E and Q_0, say to 14000 MPa and 7×10^{-4} m^2/s, respectively, then $\mathcal{P}_{cm} \approx 0.00058t$, $\mathcal{P}_{ckm} \approx 0.042$, $\mathcal{P}_{km} \approx 0.014t^{1/4}$, and the transition region is at $\xi \approx 0.998$, which is now much closer to the tip.

For the situation when the rock is impermeable, that is, for zero leak-off with $\mathcal{G}_c = 0$, we have used the same procedure to obtain an analytically matched asymptotic solution in the tip region [44]. The expansions for Ω in terms of the key parameter $\mathcal{P}_{km} := \mathcal{G}_k^3/\mathcal{G}_m$ are, for $\mathcal{P}_{km} \gg (\ll) (1-\xi)^{1/2}$, respectively,

$$\Omega \sim \mathcal{G}_k \left[C_{00}\sqrt{1-\xi^2} + C_{01}\mathcal{P}_{km}^{-1}(1-\xi) \right], \tag{4.1}$$

$$\Omega \sim \mathcal{G}_m^{1/3} \left[\bar{C}_{01}(1-\xi)^{2/3} + \mathcal{A}_1(\mathcal{P}_{km})(1-\xi)^h + \mathcal{A}_2(\mathcal{P}_{km}) \right]. \tag{4.2}$$

Hence the expansion (4.1) holds for values of ξ in the near-tip region, the expansion (4.2) holds for ξ in the intermediate-tip region, and the analysis yields

$$C_{00} = \hat{\mathcal{G}}_k \sqrt{\frac{\gamma}{2}}, \qquad C_{01} = 2\pi\lambda \frac{\hat{\mathcal{G}}_m \gamma^3}{C_{00}^2}, \qquad \bar{C}_{01} = \left\{ \frac{4\hat{\mathcal{G}}_m \lambda \gamma^3}{m(m-1)\cot \pi m} \right\}^{1/3}, \tag{4.3}$$

where $m = 2/3$. The motivation for defining the parameter $\mathcal{P}_{km}$ again follows directly from the dominant behavior expressed by balancing the exponents of δ, which becomes $\mathcal{P}_{km} \gg (\ll) (1-\xi)^{1/2}$. The expansion (4.1) is physically significant in the toughness dominated regime or valid close to the tip when $\mathcal{G}_k^3/\mathcal{G}_m \gg (1-\xi)^{1/2}$, and the expansion (4.2) corresponds to the viscosity dominated regime in which $\mathcal{G}_k^3/\mathcal{G}_m \ll (1-\xi)^{1/2}$. Previous work [24] give some of the terms in (4.1)–(4.2), but the matching is done numerically. The additional terms allow us to give an analytical expression for the matching of (4.1) and (4.2), obtained by solving for the remaining unknown coefficients $\mathcal{A}_1(\mathcal{P}_{km})$ and $\mathcal{A}_2(\mathcal{P}_{km})$, as shown in [44].

In other asymptotic limits, for example, for $\mathcal{P}_{cm} \ll (1-\xi)^{1/2}$ and $\mathcal{G}_c > \mathcal{G}_k$, one can obtain solutions which involve more than one transition region, as discussed at the start of section 3. In particular, for sufficiently large leak-off and viscosity, the solution for Ω consists of a leading order behavior with power law $(1-\xi)^{1/2}$ for ξ in the near-tip region, $(1-\xi)^{5/8}$ for an intermediate-tip region, and $(1-\xi)^{2/3}$ for values of ξ farther from the tip. In the case $\mathcal{G}_c > \mathcal{G}_k$, a transition must occur at $1-\xi = O(\mathcal{P}_{ckm}^2)$ between the near-tip square root behavior and the $(1-\xi)^{5/8}$ behavior. If, in addition, $\mathcal{P}_{cm}$ is such that $\mathcal{P}_{cm} \ll (1-\xi)^{1/2}$, then there is another transition farther from the tip at $1-\xi = O(\mathcal{P}_{cm}^2)$ between the $(1-\xi)^{5/8}$ and $(1-\xi)^{2/3}$ behavior. The construction of the nondimensionalized width Ω proceeds as in the previous sections by identifying the appropriate balance of $(1-\xi)$ with combinations of the parameters $\mathcal{G}_c$, $\mathcal{G}_k$, and $\mathcal{G}_m$. Finally, in the same way as the analysis described here in section 3.2 and in [44], we can match across the two regions to determine the unknown coefficients which are now in terms of both $\mathcal{P}_{cm}$ and $\mathcal{P}_{ckm}$.

Appendix A. Results on Π in the toughness-dominated regime.

A.1. Π_{00} is constant. Consider (3.1). We integrate to obtain

$$\Omega_{00}^3 \frac{\mathrm{d}\Pi_{00}}{\mathrm{d}z} = k_1 \tag{A.1}$$

for some constant $k_1 \neq 0$. Using the propagation condition (2.12) for Ω_{00} in (A.1) and integrating with respect to z yields

$$\Pi_{00} = -\frac{2k_1}{\hat{\mathcal{G}}_k^3 \gamma^{3/2}} z^{-1/2} + \text{ const} \tag{A.2}$$

for $z \ll 1$. Now we compare this with the result from the elasticity equation (3.2), again using the propagation condition (2.12) for Ω_{00}, to get

$$\delta^{\beta_k}\Pi_{00} = \text{const} * \int_0^{1/\delta} \frac{\mathrm{d}\Omega_{00}}{\mathrm{d}r} \frac{(1-\delta r)}{r(2-\delta r) - z(2-\delta z)}\,\mathrm{d}r = \text{ const}$$

to leading order. This contradicts (A.2) so that $k_1 = 0$. Thus, from (A.1) it follows that Π_{00} is constant.

A.2. Integration constant from the lubrication equation is zero. Integrating (3.4) with respect to z, using the leading order behavior $(2z)^{-1/2}$ for the leak-off term, gives

$$\lambda\delta^{\beta_k - 1/2}\Omega_{00} + \hat{\mathcal{G}}_c \delta^{\beta_c - 1/2}\sqrt{2} z^{1/2} + k_2 = \frac{1}{\hat{\mathcal{G}}_m \gamma^2}\Omega_{00}^3 \frac{\mathrm{d}\Pi_{01}}{\mathrm{d}z} \tag{A.3}$$

for some constant $k_2 \neq 0$. Using the propagation condition (2.12) for Ω_{00} in (A.3) and integrating with respect to z yields

$$\delta^{\sigma_1}\Pi_{01} = \frac{\hat{\mathcal{G}}_m}{\hat{\mathcal{G}}_k^3}\delta^{\beta_m - 3\beta_k}\left[\lambda\gamma\hat{\mathcal{G}}_k\delta^{\beta_k}\ln z + \sqrt{2\gamma}\hat{\mathcal{G}}_c\delta^{\beta_c}\ln z - 2\sqrt{\gamma}k_2\delta^{1/2}z^{-1/2}\right] + k_3. \tag{A.4}$$

Without loss of generality, we set the integrating constant $k_3 = 0$, as it can be incorporated into Π_{00}. We now consider the stress intensity factor K_I given in (1.2). This can be rewritten in the ξ scaling as

$$\mathcal{G}_k = \frac{8\sqrt{2}}{\pi}\gamma^{1/2}\int_0^1 \frac{\Pi}{\sqrt{1-\xi^2}}\,\mathrm{d}\xi. \tag{A.5}$$

For $\xi = 1 - \delta z$, we consider the contribution to (A.5) obtained from the term in (A.4) with coefficient k_2, namely,

$$\text{const} * \frac{8\sqrt{2}}{\pi}\gamma^{1/2}\delta^{1/2}\int_0^{1/\delta} \frac{k_2}{z\sqrt{2-\delta z}}\,\mathrm{d}z. \tag{A.6}$$

For $k_2 \neq 0$, this term is infinite at $z = 0$. So $k_2 = 0$ to maintain a finite energy.

Appendix B. Calculation of the expression for Π. We summarize the calculation of the asymptotic behavior of Π from (2.9) to find the leading order behavior. We introduce a parameter ξ^* which is in the transition region $1 - \xi = O(\mathcal{P}_{ckm}^2)$. Then the expansion (3.25) holds near the tip and (3.26) holds away from the tip, i.e.,

$$\Omega \sim \mathcal{G}_k\left[C_{00}\sqrt{1-\xi^2} + C_{01}\mathcal{P}_{km}^{-1}(1-\xi) + C_{02}\mathcal{P}_{ckm}^{-1}(1-\xi)\right] \tag{B.1}$$

for $\xi^* < \xi < 1$, and

$$\begin{aligned}\Omega \sim (\mathcal{G}_c\mathcal{G}_m)^{1/4}\Big[&\tilde{C}_{01}(1-\xi)^{5/8} + \mathcal{B}_1(\mathcal{P}_{ckm})(1-\xi)^{1/8} \\ &+ \mathcal{P}_{cm}^{-1/4}\mathcal{B}_2(1-\xi)^{3/4} + \mathcal{B}_3(\mathcal{P}_{ckm})(1-\xi)^r\Big]\end{aligned} \tag{B.2}$$

for $\xi < \xi^*$, and (2.9) becomes

(B.3)

$$\begin{aligned}\Pi =& -\frac{\mathcal{G}_k C_{00}}{4\pi\gamma}\int_{\xi^*}^1 \frac{\left[\sqrt{1-\chi^2}\right]' 2\chi \mathrm{d}\chi}{\chi^2-\xi^2} - \frac{\mathcal{G}_k\left[C_{01}\mathcal{P}_{km}^{-1}+C_{02}\mathcal{P}_{ckm}^{-1}\right]}{4\pi\gamma}\int_{\xi^*}^1 \frac{\left[(1-\chi)\right]' 2\chi \mathrm{d}\chi}{\chi^2-\xi^2}\\ &-(\mathcal{G}_c\mathcal{G}_m)^{1/4}\left\{\frac{\tilde{C}_{01}}{4\pi\gamma}\int_0^{\xi^*}\frac{\left[(1-\chi)^{5/8}\right]' 2\chi \mathrm{d}\chi}{\chi^2-\xi^2} + \frac{\mathcal{B}_1(\mathcal{P}_{ckm})}{4\pi\gamma}\int_0^{\xi^*}\frac{\left[(1-\chi)^{1/8}\right]' 2\chi \mathrm{d}\chi}{\chi^2-\xi^2}\right\}\\ &-(\mathcal{G}_c\mathcal{G}_m)^{1/4}\left\{\frac{\mathcal{P}_{cm}^{-1/4}\mathcal{B}_2}{4\pi\gamma}\int_0^{\xi^*}\frac{\left[(1-\chi)^{3/4}\right]' 2\chi \mathrm{d}\chi}{\chi^2-\xi^2} + \frac{\mathcal{B}_3(\mathcal{P}_{ckm})}{4\pi\gamma}\int_0^{\xi^*}\frac{\left[(1-\chi)^{r}\right]' 2\chi \mathrm{d}\chi}{\chi^2-\xi^2}\right\}\\ =:& \ I_1+I_2+I_3+I_4+I_5+I_6.\end{aligned}$$

In the intermediate region $1-\xi = O(\mathcal{P}_{ckm}^s)$ for $0 < s < 2$, the integrals I_1 and I_2 can be evaluated to give

$$\begin{aligned}I_1 =& \frac{\mathcal{G}_k C_{00}}{4\pi\gamma}(1+\xi)^{-1}\sqrt{2}(1-\xi^*)^{1/2}\left\{\left(1+O\big(1-\xi^*\big)\right)+O\left(\frac{1-\xi^*}{1+\xi}\right)\right\}\\ &+\frac{\mathcal{G}_k C_{00}}{4\pi\gamma}(1-\xi)^{-1}\sqrt{2}(1-\xi^*)^{1/2}\left\{\left(1+O\big(1-\xi^*\big)\right)+O\left(\frac{1-\xi^*}{1-\xi}\right)\right\},\\ I_2 =& -\frac{\mathcal{G}_k\left[C_{01}\mathcal{P}_{km}^{-1}+C_{02}\mathcal{P}_{ckm}^{-1}\right]}{4\pi\gamma}\left\{\ln\left|1-\frac{1-\xi^*}{1+\xi}\right|+\ln\left|1-\frac{1-\xi^*}{1-\xi}\right|\right\},\end{aligned} \tag{B.4}$$

while in the near-tip region $1-\xi = O(\mathcal{P}_{ckm}^s)$ for $s > 2$ the integrals are of the form

(B.5)

$$\begin{aligned}I_1 =& \frac{\mathcal{G}_k C_{00}}{4\pi\gamma}(1+\xi)^{-1}\sqrt{2}(1-\xi^*)^{1/2}\left\{\left(1+O\big(1-\xi^*\big)\right)+O\left(\frac{1-\xi^*}{1+\xi}\right)\right\}\\ &+\frac{\mathcal{G}_k C_{00}}{4\pi\gamma}\left\{\pi-\arctan\left(\frac{\xi^*}{\sqrt{1-\xi^{*2}}}\right)+\frac{\xi}{\sqrt{1-\xi^2}}\ln\left|\frac{1-\xi^*\xi+\sqrt{1-\xi^2}\sqrt{1-\xi^{*2}}}{\xi-\xi^*}\right|\right\},\\ I_2 =& -\frac{\mathcal{G}_k\left[C_{01}\mathcal{P}_{km}^{-1}+C_{02}\mathcal{P}_{ckm}^{-1}\right]}{4\pi\gamma}\left\{\ln\left|1-\frac{1-\xi^*}{1+\xi}\right|+\ln\left|\frac{1-\xi^*}{1-\xi}\right|+\ln\left|1-\frac{1-\xi}{1-\xi^*}\right|\right\}.\end{aligned}$$

We briefly outline the calculation of I_3, I_4, I_5, and I_6 for a general integral of that form with parameter $0 < a < 1$: then the results follow from setting $a = 5/8$, $1/8$, $3/4$, r, respectively. Thus the integral is

$$J_3 = \int_0^{\xi^*}(1-\chi)^{a-1}\frac{2\chi \mathrm{d}\chi}{\chi^2-\xi^2}, \tag{B.6}$$

which is now split as

$$J_3 = \int_0^{\xi^*}\frac{(1-\chi)^{a-1}}{\chi-\xi}\,\mathrm{d}\chi - \int_{-\xi^*}^0\frac{(1+\chi')^{a-1}}{\chi'-\xi}\,\mathrm{d}\chi' =: J_3^A + J_3^B. \tag{B.7}$$

Note that ξ can vary over the whole interval, i.e., $-1 < \xi < 1$. Then asymptotic expansions for the integrals are used, depending on whether ξ is inside or outside the interval of integration. It is convenient to use a change of variables which captures the asymptotic behavior of Π near the tip. It is also convenient to use different variables on different intervals, such as $\delta Z = 1-\xi$, $\delta R = 1-\chi$ in J_3^A and, $\delta Z = 1+\xi$,

$\delta R = 1 + \chi$ in J_3^B. We describe the procedure for the integral J_3^A (then J_3^B follows from an analogous calculation). This is split into three parts as

$$J_3^A = -\delta^{a-1}\left(\int_0^\infty - \int_{1/\delta}^\infty - \int_0^{(1-\xi^*)/\delta}\right)\frac{R^{a-1}}{R-Z}\,\mathrm{d}R. \tag{B.8}$$

In the intermediate region $1-\xi = O(\mathcal{P}_{ckm}^s)$ for $0 < s < 2$, the leading order behavior is determined by the first integral for $\delta = \mathcal{P}_{ckm}^2 \ll 1$ (as given in [40]), and so

$$J_3^A = (\delta Z)^{a-1}\pi\cot\pi a + O(1).$$

Then, for intermediate values of $\xi < \xi^*$, the integrals I_1, I_2, and J_3^B all give $O(1)$ contributions, which are lower order compared to the leading order term in J_3^A. The integral for J_4 is calculated in the same way. Hence the expression for Π in (B.3) is

$$\begin{aligned}\Pi = (\mathcal{G}_c\mathcal{G}_m)^{1/4}&\left\{\frac{q\tilde{C}_{01}}{4\pi\gamma}(1-\xi)^{q-1}\pi\cot\pi q + \frac{g\mathcal{B}_1(\mathcal{P}_{ckm})}{4\pi\gamma}(1-\xi)^{g-1}\pi\cot\pi g\right\}\\ &+(\mathcal{G}_c\mathcal{G}_m)^{1/4}\left\{\frac{p\mathcal{P}_{cm}^{-1/4}\mathcal{B}_2}{4\pi\gamma}(1-\xi)^{p-1}\pi\cot\pi p\right.\\ &\left.+\frac{r\mathcal{B}_3(\mathcal{P}_{ckm})}{4\pi\gamma}(1-\xi)^{r-1}\pi\cot\pi r\right\} + O(1),\end{aligned}$$

where $q = 5/8$, $g = 1/8$, $p = 3/4$ and the $O(1)$ terms are higher order with respect to $1-\xi \ll 1$.

Similarly, for values of ξ in the near-tip region $1-\xi = O(\mathcal{P}_{ckm}^s)$ for $s > 2$, the integral I_3 gives $O(1)$ contributions, and the leading order term is the singularity in I_2 defined in (B.5). Hence the expression for Π is now

$$\begin{aligned}\Pi = \mathcal{G}_k&\left[\frac{C_{00}}{4\gamma} - \frac{C_{01}\mathcal{P}_{km}^{-1} + C_{02}\mathcal{P}_{ckm}^{-1}}{4\pi\gamma}\left\{\ln\left|1-\frac{1-\xi^*}{1+\xi}\right| + \ln\left|\frac{1-\xi^*}{1-\xi}\right| + \ln\left|1-\frac{1-\xi}{1-\xi^*}\right|\right\}\right]\\ &+O(1).\end{aligned}$$

Here we have explicitly included the leading order term from I_1 for comparison with (3.31). Additional error terms not shown here also result from the fact that higher order derivatives for $\Omega(\xi)$ are not matched in the transition region: these can be shown to be higher order for $\mathcal{P}_{ckm} \ll 1$.

Acknowledgments. We would like to thank Emmanuel Detournay, José Adachi, and Dmitry Garagash for their very helpful comments and for sharing a number of preprints with us.

REFERENCES

[1] H. Abé, T. Mura, and L. M. Keer, *Growth rate of a penny-shaped crack in hydraulic fracturing of rocks*, J. Geophys. Res., 81 (1976), pp. 5335–5340.

[2] J. I. Adachi and E. Detournay, *Self-similar solution of a plane-strain fracture driven by a power-law fluid*, Int. J. Numer. Anal. Meth. Geomech., 26 (2002), pp. 579–604.

[3] J. I. Adachi and E. Detournay, *Plane-strain propagation of a fluid-driven fracture: Finite toughness self-similar solution*, in preparation, 2006.

[4] J. I. Adachi and E. Detournay, *Propagation of a fluid-driven fracture in a permeable medium*, J. Eng. Fracture Mech., submitted, 2006.

[5] J. I. Adachi, E. Siebrits, A. Peirce, and J. Desroches, *Computer simulation of hydraulic fractures*, Int. J. Rock Mech. and Min. Sci., submitted, 2006.
[6] J. I. Adachi, *Fluid-Driven Fracture in Permeable Rock*, Ph.D. Thesis, University of Minnesota, 2001; available at www.umi.com.
[7] S. H. Advani, T. S. Lee, and J. K. Lee, *Three-dimensional modeling of hydraulic fractures in layered media: Finite element formulations*, ASME J. Energy Res. Technol., 112 (1990), pp. 1–18.
[8] G. Barenblatt, *The mathematical theory of equilibrium cracks in brittle fracture*, Adv. Appl. Mech., 7 (1962), pp. 55–129.
[9] A. P. Bunger, E. Detournay, and D. I. Garagash, *Toughness-dominated regime with leak-off*, Int. J. Fracture, 134 (2005), pp. 175–190.
[10] R. S. Carbonell, J. Desroches, and E. Detournay, *A comparison between a semi-analytical and a numerical solution of a two-dimensional hydraulic fracture*, Internat. J. Solids Structures, 36 (1999), pp. 4869–4888.
[11] E. Carter, *Optimum fluid characteristics for fracture extension*, in Drilling & Production Practices, G. Howard and C. Fast, eds., American Petroleum Institute, Tulsa, OK, 1957, pp. 261–270.
[12] R. J. Clifton and A. S. Abou-Sayed, *A variational approach to the prediction of the three-dimensional geometry of hydraulic fractures*, in Proceedings of the SPE/DOE Low Permeability Reservoir Symposium, Denver, CO, 1981.
[13] B. Cotterell and J. R. Rice, *Slightly curved or kinked cracks*, Internat. J. Fracture, 16 (1980), pp. 155–169.
[14] B. C. Crittendon, *The mechanics of design and interpretation of hydraulic fracture treatments*, J. Pet. Tech. 11, October 1959, pp. 21–29.
[15] J. Desroches, E. Detournay, B. Lenoach, P. Papanastasiou, J. R. A. Pearson, M. Thiercelin, and A. H.-D. Cheng, *The crack tip region in hydraulic fracturing*, Proc. R. Soc. London Ser. A, 447 (1994), pp. 39–48.
[16] E. Detournay, J. I. Adachi, and D. I. Garagash, *Asymptotic and intermediate asymptotic behavior near the tip of a fluid-driven fracture propagating in a permeable elastic medium*, in Structural Integrity and Fracture, A. V. Dyskin, X. Hu, and E. Sahouryeh, eds., Swets & Zeitlinger, Lisse, Zuid-Holland, The Netherlands, 2002.
[17] E. Detournay and A. H.-D. Cheng, *Plane strain analysis of a stationary hydraulic fracture in a poroelastic medium*, Internat. J. Solids Structures, 27 (1991), pp. 1645–1662.
[18] E. Detournay and A. H.-D. Cheng, *Fundamentals of Poroelasticity*, in Comprehensive Rock Engineering, Principles, Practice & Projects, Vol. 2, J. A. Hudson, ed., Pergamon Press, Oxford, UK, 1993, Chap 5, pp. 113–169.
[19] E. Detournay and D. I. Garagash, *The near-tip region of a fluid-driven fracture propagating in a permeable elastic solid*, J. Fluid Mech., 494 (2003), pp. 1–32.
[20] E. Detournay and D. I. Garagash, *General scaling laws for fluid-driven fractures*, preprint, 2004.
[21] E. Detournay, *Propagation regimes of of fluid-driven fractures in impermeable rocks*, Int. J. Geomech., 4 (2004), pp. 1–11.
[22] A. V. Dyskin, L. N. Germanovich, and K. B. Ustinov, *Asymptotic analysis of crack interaction with free boundary*, Internat. J. Solids Structures, 37 (2000), pp. 857–886.
[23] D. I. Garagash, E. Detournay, and J. I. Adachi, *Tip solution of a fluid-driven fracture in a permeable rock*, in preparation, 2006.
[24] D. I. Garagash and E. Detournay, *Plane-strain propagation of a fluid-driven fracture: Small toughness solution*, J. Appl. Mech., 72 (2005), pp. 916–928.
[25] D. I. Garagash, *Hydraulic fracture propagation in elastic rock with large toughness*, in Proceedings of the 4th North American Rock Mechanics Symposium, J. Girard, M. Liebman, C. Breeds, and T. Doe, eds., 2000, pp. 221–228.
[26] D. I. Garagash, *Plane-strain propagation of a hydraulic fracture during injection and shut-in: Asymptotics of large toughness*, Engrg. Fracture Mech., 73 (2006), pp. 456–481.
[27] D. Garagash and E. Detournay, *The tip region of a fluid-driven fracture propagating in an elastic medium*, ASME J. Appl. Mech., 67 (2000), pp. 183–192.
[28] J. Geertsma and F. de Klerk, *A rapid method of predicting width and extent of hydraulically induced fractures*, J. Pet. Technol., 246 (1969), pp. 1571–1581.
[29] Y. N. Gordeyev and V. M. Entov, *The pressure distribution around a growing crack*, J. Appl. Math. Mech., 61 (1997), pp. 1025–1029.
[30] E. Harrison, W. F. Kieschnick, and W. J. McGuire, *The mechanics of fracture induction and extension*, Petroleum Trans. AIME, 201 (1954), pp. 252–263.
[31] G. C. Howard and C. R. Fast, *Optimum fluid characteristics for fracture extension*, Drilling and Production Practice, 24 (1957), pp. 261–270.

[32] M. K. Hubbert and D. G. Willis, *Mechanics of hydraulic fracturing*, Pet. Trans. (AIME), 210 (1957), pp. 153–166.
[33] S. Khristianovic and Y. Zheltov, *Formation of vertical fractures by means of highly viscous fluids*, in Proceedings of the 4th World Petroleum Congress, Rome, Italy, 1955, pp. 579–586.
[34] O. Kresse, E. Detournay, and D. I. Garagash, *Universal tip solution for a fracture driven by a power law fluid*, preprint (to be submitted to J. Non-Newtonian Fluid Mech.), 2005.
[35] O. Kresse and E. Detournay, *Tip solution for a fracture driven by a perfectly plastic fluid*, preprint (to be submitted to J. Elasticity), 2005.
[36] B. Lenoach, *The crack tip solution for hydraulic fracturing in a permeable solid*, J. Mech. Phys. Solids, 43 (1995), pp. 1025–1043.
[37] J. R. Lister, *Buoyancy-driven fluid fracture: similarity solutions for the horizontal and vertical propagation of fluid-filled cracks*, J. Fluid Mech., 217 (1990), pp. 213–239.
[38] J. R. Lister, *Buoyancy-driven fluid fracture: The effects of material toughness and of low-viscosity precursors*, J. Fluid Mech., 210 (1990), pp. 263–280.
[39] M. G. Mack and N. R. Warpinski, *Mechanics of hydraulic fracturing*, in Reservoir Stimulation, 3rd ed., M. Economides and K. Nolte, eds., John Wiley & Sons, New York, Chap. 6, 2000.
[40] P. A. Martin, *End-point behaviour of solutions to hypersingular integral equations*, Proc. Roy. Soc. London Ser. A, 432 (1991), pp. 301–320.
[41] P. A. Martin, *Perturbed cracks in two dimensions: An integral-equation approach*, Internat. J. Fracture, 104 (2000), pp. 317–327.
[42] P. A. Martin, *On wrinkled penny-shaped cracks*, J. Mech. Phys. Solids, 49 (2001), pp. 1481–1495.
[43] S. L. Mitchell, R. Kuske, A. P. Peirce, and J. I. Adachi, *An asymptotic analysis of a finger-like fluid-driven fracture*, in preparation, 2006.
[44] S. L. Mitchell, R. Kuske, and A. P. Peirce, *An asymptotic framework for the analysis of hydraulic fractures: The impermeable case*, J. Appl. Mech., in press (preprint available at www.iam.ubc.ca/∼sarah/), 2007.
[45] R. Nordgren, *Propagation of vertical hydraulic fractures*, SPE J., 12 (1972), pp. 306–314.
[46] A. P. Peirce and E. Siebrits, *The scaled flexibility matrix method for the efficient solution of boundary value problems in* $2d$ *and* $3d$ *layered elastic media*, Comput. Methods Appl. Mech. Engrg., 1990 (2001), pp. 5935–5956.
[47] A. P. Peirce and E. Siebrits, *An efficient multilayer planar* $3d$ *fracture growth algorithm using a fixed mesh approach*, Internat. J. Numer. Methods Engrg., 53 (2002), pp. 691–717.
[48] T. K. Perkins and L. R. Kern, *Widths of hydraulic fractures*, J. Pet. Tech., 222 (1961), pp. 937–949.
[49] J. R. Rice, *Mathematical analysis in the mechanics of fracture*, in Fracture, an Advanced Treatise, Vol. 2, Academic Press, New York, 1968, Chap. 3, pp. 191–311.
[50] A. A. Savitski and E. Detournay, *Propagation of a penny-shaped fluid-driven fracture in an impermeable rock: Asymptotic solutions*, Internat. J. Solids Structures, 39 (2002), pp. 6311–6337.
[51] A. Settari, *A new general model of fluid loss in hydraulic fracturing*, Soc. Pet. Engrg. J., 4 (1985), pp. 491–501.
[52] I. Sneddon and Lowengrub M, *Crack Problems in the Classical Theory of Elasticity*, John Wiley & Sons, New York, 1969.
[53] J. L. S. Sousa, B. J. Carter, and A. R. Ingraffea, *Numerical simulation of* $3d$ *hydraulic fracturing using Newtonian and power-law fluids*, Int. J. Rock Mech. Min. Sci., 30 (1993), pp. 1265–1271.
[54] D. A. Spence and P. Sharp, *Self-similar solutions for elastohydrodynamic cavity flow*, Proc. Roy. Soc. London Ser. A, 400 (1985), pp. 289–313.
[55] D. A. Spence and D. L. Turcotte, *Magma-driven propagation of cracks*, J. Geophys. Res., 90 (1985), pp. 575–580.